Slow-Wave Half-Mode Substrate Integrated Waveguide Using Spoof Surface Plasmon Polariton Structure

Dong-Fang Guan, Peng You, Qingfeng Zhang, Zhang-Biao Yang, Haiwen Liu, and Shao-Wei Yong

***Abstract*— In this paper, we propose a novel slow-wave half-mode substrate integrated waveguide (HMSIW) combined with spoof surface plasmon polariton (SPP) structure. In this design, subwavelength corrugated grooves are etched on the up metal layer of HMSIW to support an SPP mode. The dispersion and transmission characteristics of the proposed hybrid HMSIW-SPP structure are analyzed and compared with the classic HMSIW. To experimentally validate this design, a prototype is fabricated and measured. A slow-wave effect is clearly observed in the proposed hybrid transmission line, and its wavelength is reduced by over 50% without sacrificing its transmission performance. This structure features a simple architecture and excellent slow-wave effect.**

***Index Terms*— Half-mode substrate integrated waveguide (HMSIW), slow-wave effect, surface plasmon polariton (SPP).**

I. Introduction

SUBSTRATE integrated waveguide (SIW) is a competitive transmission line (TL) since it has the merits of both planar TL and metallic rectangular waveguide [1], [2]. Through digging two rows of metallic via holes on a printed circuit board (PCB) substrate, SIW has the similar performance to metallic waveguide i.e., low insertion loss, low interference, and low radiation. Moreover, it can be easily integrated with other planar circuits. Recently, SIW has been applied to the design of many high-quality microwave and millimeter-wave components. However, the size of SIW is too large in comparison with other planar TLs [3]. It is highly demanded to reduce the size of SIW and hence to improve the compactness of SIW circuits, especially for low-frequency applications.

The concept of half-mode SIW (HMSIW) was proposed in [3], where it is formed by bisecting SIW along a fictitious quasi-magnetic wall. HMSIW preserves the field distribution of the original SIW and hence maintains all the superiorities with half size only [4]. Another way to reduce the transverse size of SIW is to develop folded SIW (FSIW) [5]–[7]. Using double-layer substrate, the height of FSIW was improved, but the width was reduced to about one-half of the initial one. Ridge SIW using metallic blind holes at the center of the SIW was also employed in [8], where the width was reduced by 40%. All of the aforementioned miniaturization technologies are focused on the reduction of the transverse dimension for SIW. To reduce the longitudinal dimension, one may use a slow-wave structure, which has a shorter wavelength [9]–[11]. The concept of slow-wave SIW was proposed in [12]. By adding several rows of metallic blind holes on the substrate, the SIW achieved a slow-wave effect, leading to 40% reduction of both transverse and longitudinal dimensions. In [13], another slow-wave SIW patterned with microstrip polyline was presented. A size reduction of 40% for both longitudinal and transverse dimensions was achieved in comparison with the original SIW. It was proven that introducing slow-wave feature to SIW TLs and devices improves their compactness in longitudinal dimension or realizes some functionality. Based on the designs of [12] and [13], slow-wave HMSIW components were also developed in [14] and [15].

Surface plasmon polariton (SPP) is a special kind of surface electromagnetic wave propagating along the surface of a conductor at optical frequencies with the advantage of confining light in a subwavelength scale [16]. By using the periodical subwavelength structure to mimic the characteristics of SPP, spoof SPP was realized in microwave frequency [17]. In previous works, spoof SPPs were designed mainly based on 3-D metallic structures by decorating with subwavelength grooves or holes [18]–[20]. Recently, a novel planar strip TL with subwavelength corrugated structure was proposed to support and propagate surface plasmon modes on electrically ultrathin and flexible films [21]. This opens a new way to develop planar spoof SPPs. Due to high field confinement and slow-wave feature, spoof SPP has inspired much research interest in the design of microwave and millimeter-wave devices, including TLs [22]–[24], filters [25], [26], and antennas [27]–[29]. A hybrid SIW-SPP slow-wave transmission structure was proposed in [30], where SPP structure was constituted inside the SIW through employing arrays of transverse metallic blind holes. Such a structure needs a thick substrate to allow high via holes to produce a large slow-wave effect and hence is not suitable for compact circuit applications.

Manuscript received July 23, 2017; revised November 4, 2017, January 23, 2018, and March 10, 2018; accepted March 30, 2018. Date of publication May 1, 2018; date of current version June 4, 2018. This work was supported in part by the Natural Science Foundation of Hunan Province, China, under Grant 2017JJ3364, in part by the National Natural Science Foundation of China under Grant 61601487, in part by the Guangdong NSF for DYS under Grant 2015A030306032, and in part by the Guangdong STD Funds under Grant 2016TQ03X839. *(Corresponding authors: Peng You; Qingfeng Zhang.)*

D.-F. Guan, P. You, Z.-B. Yang, and S.-W. Yong are with the College of Electronic Science and Engineering, National University of Defense Technology, Changsha 410073, China (e-mail: gdfguandongfang@163.com; ypnudt@126.com).

Q. Zhang is with the Department of Electronics and Electrical Engineering, Southern University of Science and Technology, Shenzhen 518055, China (e-mail: zhang.qf@sustc.edu.cn).

H. Liu is with the School of Electronic and Information Engineering, Xi'an Jiaotong University, Xi'an 710049, China.

Color versions of one or more of the figures in this paper are available online at http://ieeexplore.ieee.org.

Digital Object Identifier 10.1109/TMTT.2018.2825385

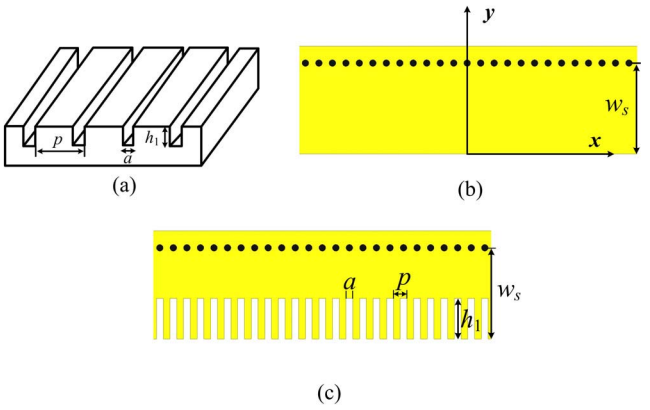

Fig. 1. Configurations of (a) SPP, (b) HMSIW, and (c) proposed HMSIW-SPP.

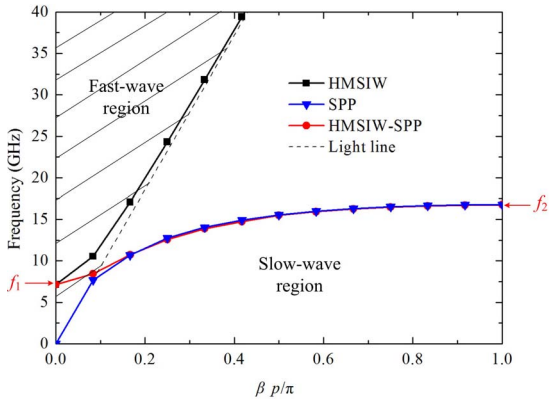

Fig. 2. Dispersion diagrams comparison.

Furthermore, it is difficult and complicated to produce metalized blind via holes in the fabrication.

In this paper, we propose a new slow-wave HMSIW based on purely planar spoof SPP structures. By etching subwavelength corrugated grooves on the up metal layer of HMSIW, the proposed hybrid HMSIW-SPP structure achieves a slow-wave effect using a thin substrate. It employs a purely planar corrugation instead of the nonplanar blind via holes used in [30]. Therefore, this HMSIW-SPP features simpler structure and easier fabrication in comparison with the structure in [30]. The dispersion and transmission characteristics of the proposed slow-wave HMSIW-SPP structure are analyzed and simulated. Simulation results indicate that the slow-wave effect is obvious and the wavelength is reduced more than 50% in comparison with the conventional HMSIW.

This paper is organized as follows. The configuration and characteristics analysis of the proposed hybrid HMSIW-SPP structure are presented in Section II. Section III describes the experimental validation and discussion. Conclusions are drawn in Section IV.

II. Principle of Slow-Wave HMSIW With SPP Structure

A. Configuration

Fig. 1 shows the configurations of typical SPP, HMSIW, and the proposed hybrid HMSIW-SPP structure. As shown in Fig. 1(a), the grooves are corrugated in a perfect conductor to construct an ideal spoof SPP structure. The width and depth of grooves are a and h_1, respectively, and the period of the SPP element is p. One should note that such a structure has an infinite transversal width, which is not available in practice. The dispersion relation of this ideal SPP is

$$\beta = k_0\sqrt{1+\frac{a^2}{p^2}\tan^2(k_0h_1)} \tag{1}$$

where β is the propagation constant and $k_0 = \omega/c$.

As shown in Fig. 1(b), HMSIW uses a row of metallic via holes on one side (mimicking an electric wall) and leaves open on the other side (mimicking a quasi-magnetic wall). The width of this waveguide is w_s. HMSIW preserves the field distribution of the original SIW and hence all its superiorities with only half of the transversal width. In order to reduce the longitudinal dimension, a novel slow-wave HMSIW with SPP structure is presented in Fig. 1(c), where spoof SPP structure formed by a subwavelength corrugated structure is added to the up metal layer of HMSIW. The period of the SPP structure unit, the width, and the depth of SPP grooves are also presented as p, a, and h_1, respectively. One should note that although such a planar spoof SPP is different from the ideal SPP in Fig. 1(a), both of them has similar characteristics. Therefore, one may use (1) to get a rough data for understanding the principle and then use a full-wave simulation to calculate the exact dispersion curve. Such planar periodic grooves can support and propagate a slow-wave mode at microwave frequencies, when a and p are much less than the wavelength at the operational frequency.

B. Slow-Wave Effect

To demonstrate the slow-wave effect of the proposed novel HMSIW structure, its dispersion characteristic is analyzed using commercial EM software Ansoft HFSS. In simulation, the model is established on a single-layered F4BM-2 PCB with thickness $h = 0.5$ mm, relative dielectric constant $\varepsilon_r = 2.65$, and loss tangent $\tan\delta = 0.001$. The parameters are set as: $w_s = 6.5$ mm; $a = 0.5$ mm; $p = 1$ mm; and $h_1 = 3$ mm. Eigen mode analysis tool of Ansoft HFSS is used to simulate the dispersion characteristics of the unit cell. The simulated dispersion diagrams are depicted in Fig. 2, in which the dispersion curves of pure HMSIW, pure spoof SPP, and hybrid HMSIW-SPP structures with identical parameters are compared. It is noted that the pure spoof SPP structure is the strip line with one side subwavelength corrugated grooves presented in [21]. According to Fig. 2, the dispersion curve of HMSIW starts at a cutoff frequency f_1 and then goes closely above the light line as the frequency increases. On the contrary, the dispersion curve of the spoof SPP structure starts at zero and matches with the light line at the beginning and then gradually goes away from it as the frequency increases until an upper cutoff frequency f_2. It indicates that HMSIW supports a pure fast-wave fundamental mode and spoof SPP structure supports a pure slow-wave mode. The proposed

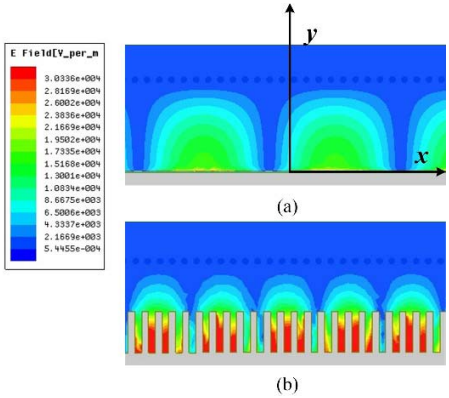

Fig. 3. Top view of E-field distributions at 12 GHz. (a) HMSIW. (b) Proposed HMSIW-SPP structure.

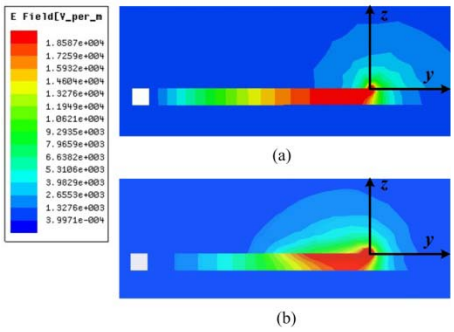

Fig. 4. Cross-sectional view of E-field distributions (total fields) at 12 GHz. (a) HMSIW. (b) Proposed HMSIW-SPP structure.

hybrid HMSIW-SPP structure exhibits the dispersion features of both HMSIW and spoof SPP, supporting a hybrid fast-wave and slow-wave modes. Its dispersion curve starts at the lower cutoff frequency f_1 at the fast-wave region and then enters into the slow-wave region and cuts off at frequency f_2. It behaves like an HMSIW at low frequencies and a spoof SPP structure at high frequencies. Therefore, slow-wave effect is obtained by applying subwavelength corrugation to the HMSIW.

The electric field and magnetic field distributions of the proposed hybrid HMSIW-SPP structure and a typical HMSIW are simulated and compared. It is noted that all the values of electric and magnetic fields are the magnitudes of total fields. Fig. 3 shows the E-field distribution along the top surface at 12 GHz. According to Fig. 2, the normalized propagation constants are 0.1 for HMSIW and 0.22 for HMSIW-SPP structure at this frequency. It is observed that the wavelength of the hybrid HMSIW-SPP structure is significantly reduced in comparison with that of HMSIW. A reduction of more than 50% is achieved in the longitudinal direction. The cross-sectional views of E-field and H-field distributions are compared in Figs. 4 and 5, respectively. For the electric field, it is mainly concentrated at the open side of both HMSIW and hybrid HMSIW-SPP structures. For the magnetic field, however, the strongest point stays away from the open side in the hybrid HMSIW-SPP structure, whereas it still concentrates at the open side in the HMSIW. It turns out that the electric and magnetic fields are separated in hybrid HMSIW-SPP structure, which is typically observed in slow-wave structures [13].

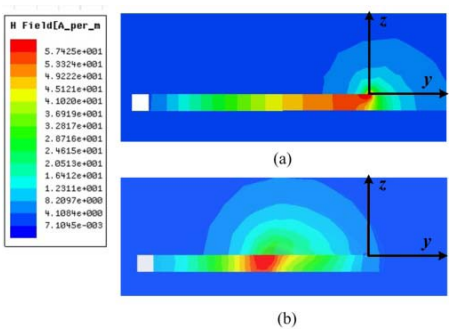

Fig. 5. Cross-sectional view of H-field distributions (total fields) at 12 GHz. (a) HMSIW. (b) Proposed HMSIW-SPP structure.

C. Parametric Study

Based on the above analysis, a slow-wave transmission feature is achieved for the HMSIW by introducing SPP structure. To analyze the influence of the geometry change on the slow-wave effect, a parametric study is conducted. The dispersion diagrams with different parameter variations are presented in Fig. 6. One should note that, when one parameter changes in the simulation, other parameters maintain the initial values. Fig. 6(a) shows the influence of the depth of grooves h_1 on the dispersion curves. As h_1 increases, propagation constant β becomes larger at the same frequency and the upper cutoff frequency is reduced, while the lower cutoff frequency remains the same. Since the phase velocity v_p is inversely proportional to propagation constant β, the phase velocity gets slower with larger h_1. The dispersion curves with different SPP periods p are shown in Fig. 6(b). It can be seen that the propagation constant β is not remarkably by the variation of parameter p. The physical reason is that the equivalent series capacitance due to the corrugation is too large in comparison with the equivalent series inductance contributed by the rest of the metal in the unit cell. Therefore, a slight change of p, in equivalence to changing the series inductance of the unit cell, does not affect the dispersion curve remarkably. Fig. 6(c) gives the simulated dispersion diagrams for different HMSIW widths w_s. It is observed that w_s has influence on the lower cutoff frequency only, and the slow-wave effect is not affected. The physical reason is that, in the slow-wave region, most of the fields are concentrated in the corrugation part, as shown in Fig. 3. The change of width does not perturb the fields and hence does not affect the dispersion curve. Furthermore, the effect of substrate thickness h is also considered. Fig. 6(d) shows that the dispersion curves for different h are nearly overlapped, which reveals that the slow-wave effect is not affected by the thickness. Slow-wave HMSIW can be designed with different thicknesses.

D. Transmission Analysis

Since the proposed hybrid HMSIW-SPP structure cannot be directly excited, an efficient conversion from conventional HMSIW is needed for its application in TL or other devices. Fig. 7 shows the configuration of the hybrid HMSIW-SPP including transitions from microstrip to HMSIW and from HMSIW to hybrid HMSIW-SPP. The whole length of the TL

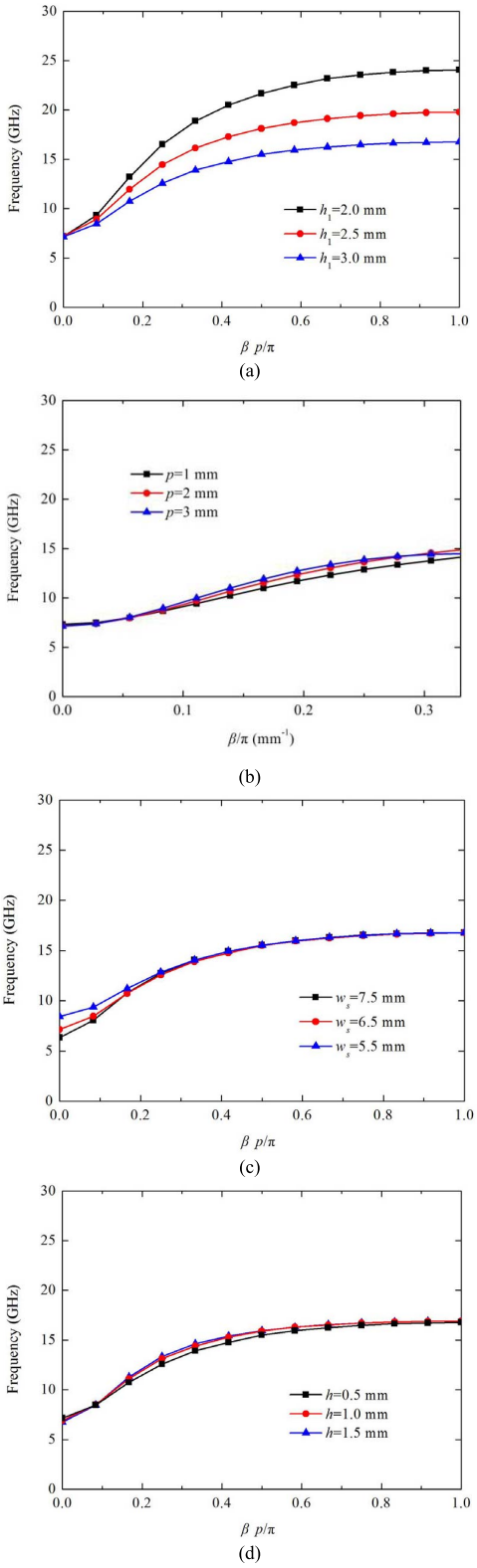

Fig. 6. Simulated dispersion diagrams of the proposed HMSIW-SPP structure with different (a) heights of SPP, (b) periods of SPP, (c) widths of HMSIW, and (d) thicknesses of substrate.

L is 80 mm, and the length of HMSIW part L_1 is 60 mm. The transition section between HMSIW and hybrid HMSIW-SPP uses a gradually varied corrugation depth (from 0.1 h_1 to h_1 with a linear gradient). Moreover, HMSIW is transited to

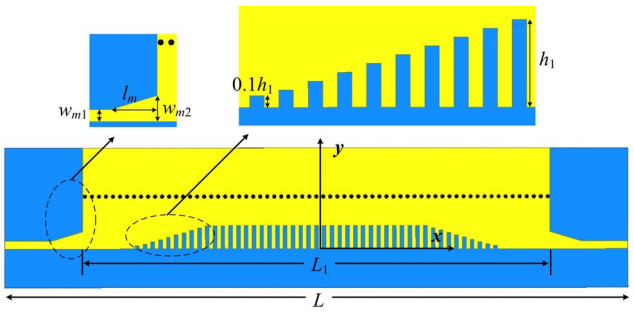

Fig. 7. Configuration of HMSIW-SPP.

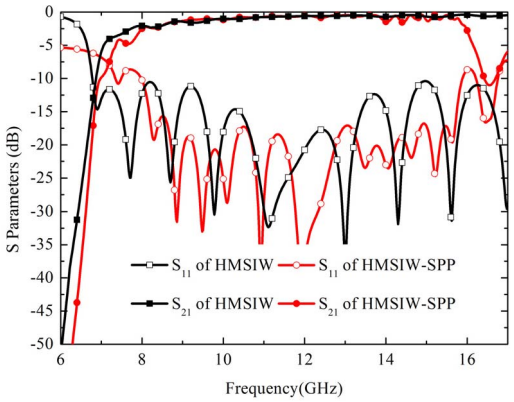

Fig. 8. Simulated reflection coefficients (S_{11}) and transmission coefficients (S_{21}) of HMSIW and the proposed HMSIW-SPP.

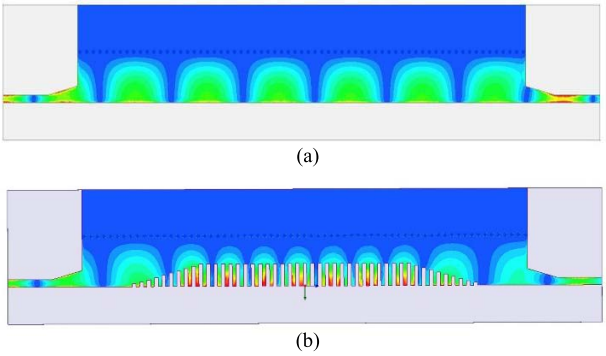

Fig. 9. E-field distributions of (a) HMSIW and (b) proposed HMSIW-SPP structure.

microstrip lines for experimental measurement. As shown in Fig. 7, the width of the microstrip lines w_{m1} is 1 mm with the characteristic impedance of 50 Ω. The width and length of the tapered microstrip lines are set as $w_{m2} = 2.2$ mm and $l_m = 3.5$ mm for impedance matching.

Fig. 8 compares the simulated reflection coefficients (S_{11}) and transmission coefficients (S_{21}) of HMSIW and hybrid HMSIW-SPP with the same length. Note that the transmission magnitude of hybrid HMSIW-SPP agrees well with that of HMSIW until it reaches up to the upper cutoff frequency. The lower and upper cutoff frequencies agree well with the dispersion curve of the unit cell in Fig. 2. The operational frequency band can be easily adjusted by tuning the parameters of SPP. Fig. 9 compares the E-field distributions of the two TLs.

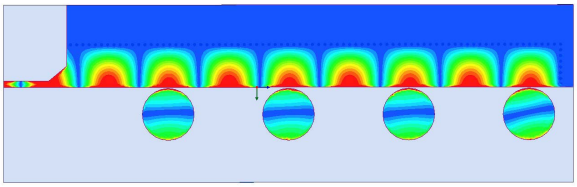

(a)

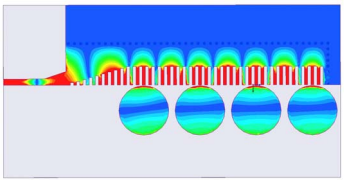

(b)

Fig. 10. Designed antenna arrays fed by (a) HMSIW and (b) HMSIW-SPP.

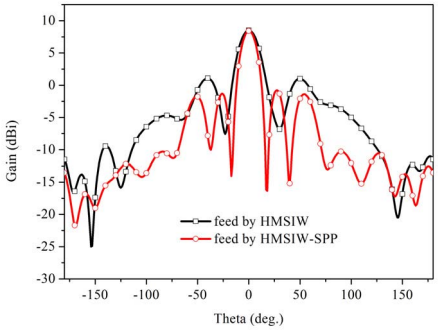

Fig. 11. Simulated gains of the antenna arrays fed by HMSIW and HMSIW-SPP at 12 GHz.

Note that the electric fields are highly concentrated and located at the edge of the corrugated surface in HMSIW-SPP.

To show the advantage of HMSIW-SPP over HMSIW, we apply the two structures to series-fed antenna arrays for broadside radiation. As shown in Fig. 10, a row of four-circular metallic patches are set as the radiating elements and fed by TLs through coupled feeding, like the design in [27]. To achieve a broadside radiation, each antenna element should be excited in phase. Due to the fact that HMSIW-SPP has a smaller guided wavelength than HMSIW, the space between adjacent elements in Fig. 10(b) is much smaller. Except the microstrip part, the longitudinal size of the HMSIW-SPP-fed antenna array is reduced 50%. Fig. 11 shows the simulated gains of the antenna arrays fed by HMSIW and HMSIW-SPP at 12 GHz. It can be seen the gains are in the same level. This comparison well demonstrates the advantage of HMSIW-SPP.

III. Experimental Results and Discussion

To validate the proposed hybrid HMSIW-SPP, a prototype is fabricated and measured. Fig. 12 shows the photograph of fabricated prototype. The physical size of the whole TL is 80 $\times$ 18 mm^2. One should note that we do not use any de-embedding technique for the simulation and measurement results. In other words, all the results include both HMSIW-SPP TL and transitions. Fig. 13 presents the measured and simulated magnitude curves of the reflection

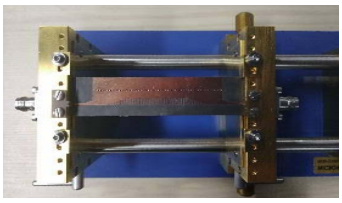

Fig. 12. Photograph of the HMSIW-SPP structure.

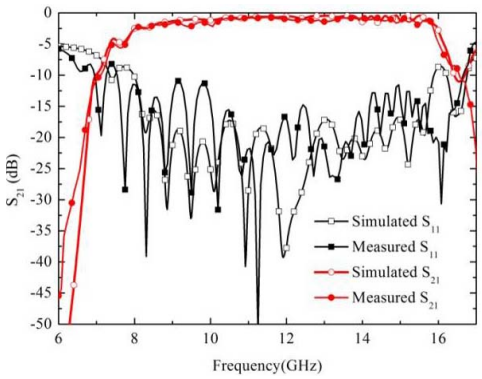

Fig. 13. Measured and simulated reflection coefficients (S_{11}) and transmission coefficients (S_{21}) of the proposed HMSIW-SPP.

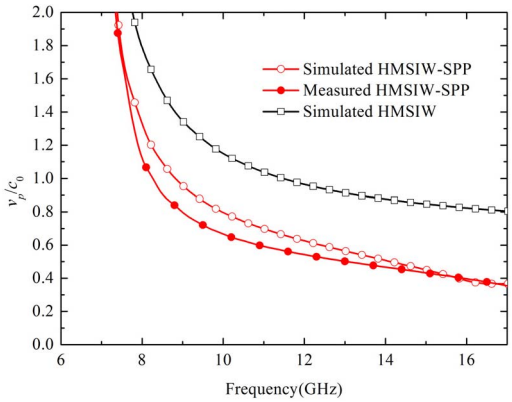

Fig. 14. Measured and simulated phase velocities of the proposed HMSIW-SPP.

coefficients (S_{11}) and transmission coefficients (S_{21}). The measured responses agree well with the simulated ones, despite of a slightly higher reflection around 10 GHz due to the fabrication tolerance. The insertion losses of the simulated and measured S_{21} are 0.56 and 1.02 dB at 12 GHz, respectively. The measured insertion loss higher than the simulated one may be attributed to a higher loss tangent used in the fabricated substrate than the simulated one. Fabricated tolerance also contributes to the difference between the two.

The measured and simulated phase curves of hybrid HMSIW-SPP are shown in Fig. 14. Note that the trend of the two curves is consistent. The difference between measured and simulated phase velocities is mainly caused by the fabrication tolerances. For convenience, the velocities are normalized with light speed in the air c_0. It is observed that the phase velocity of the proposed hybrid HMSIW-SPP is slower than

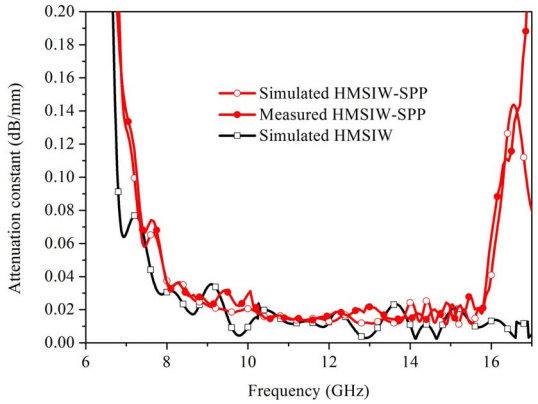

Fig. 15. Measured and simulated attenuation constants of the proposed HMSIW-SPP.

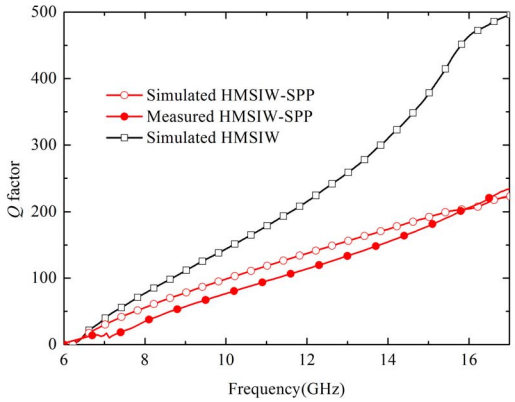

Fig. 16. Measured and simulated Q factors of the proposed HMSIW-SPP.

that of HMSIW. One should note that, since the calculated phase velocity here also includes the contributions from the transition parts, the pure HMSIW-SPP should get even slower. The measured and simulated attenuation constants and Q factors of the proposed hybrid HMSIW-SPP are also presented and compared with HMSIW as shown in Figs. 15 and 16. The simulated attenuation constants of HMSIW-SPP and conventional HMSIW are almost at the same level. The measured attenuation constant is 0.016 dB/mm at the passband center. The measured and simulated Q factors of HMSIW-SPP are 114 and 137 at 12 GHz, while the simulated one of HMSIW is 215.

Table I compares the proposed HMSIW-SPP with some representative slow-wave SIWs. First, all the slow-wave TLs have notable longitudinal reduction due to the slow-wave effect. Note that the slow-wave effect can be adjusted in some extent by tuning parameters for all the designs. Second, the lower cutoff frequency is not affected by introducing SPP, and hence, no lateral reduction is achieved in our design. However, the lateral physical size of HMSIW has already reduced by 50% in comparison with SIW used in [12] and [13]. Third, the attenuation constant in our design is the least. The reason is that our work has the simplest structure compared with other slow-wave SIWs. Double layers are needed in [12] for digging blind via holes, leading to more complicated fabrications.

TABLE I
PERFORMANCE COMPARISON OF DIFFERENT SIW SLOW-WAVE STRUCTURES

	Frequency (GHz)	Longitudinal reduction (%)	Lateral reduction (%)	Attenuation constant (dB/mm)	No. of Layer	Type
[12]	12	40	40	0.03	2	SIW with blind via holes
[13]	12	40	40	0.02	1	SIW with microstrip polyline
Our work	12	>50	50	0.016	1	HMSIW with SPP structure

Microstrip polyline is also difficult to be optimized in [13]. While SPP structure used in our design is only 1-D structure, it is easily designed and adjusted to realize different slow-wave effects.

IV. CONCLUSION

In this paper, we have proposed a hybrid HMSIW-SPP structure to slow down the phase velocity in HMSIW. The dispersion characteristics of the proposed HMSIW-SPP unit was simulated and analyzed. It revealed that the hybrid HMSIW-SPP structure had excellent slow-wave effect. Besides, the proposed HMSIW-SPP structure was designed and compared with a conventional HMSIW. The simulation results indicated that the proposed TL has a smaller wavelength and slower phase velocity. Finally, a sample of the slow-wave structure was fabricated and measured. According to the performance comparison with other SIW slow-wave structures, the proposed design is attractive due to its simple structure and excellent slow-wave effect.

REFERENCES

[1] K. Wu, D. Deslandes, and Y. Cassivi, "The substrate integrated circuits—A new concept for high-frequency electronics and optoelectronics," in *Proc. 6th Int. Conf. Telecommun. Modern Satellite, Cable Broadcasting Service (TELSIKS)*, vol. 1. Oct. 2003, pp. P-III–P-X.

[2] W. Hong *et al.*, "SIW-Like guided wave structures and applications," *IEICE Trans. Electron.*, vol. E92-C, no. 9, pp. 1111–1123, 2009.

[3] W. Hong *et al.*, "Half mode substrate integrated waveguide: A new guided wave structure for microwave and millimeter wave application," in *Proc. Joint 31st Int. Infr. Millim. Wave Conf. 14th Int. Terahertz Electron. Conf.*, Shanghai, China, Sep. 2006, p. 219.

[4] Q. Lai, C. Fumeaux, W. Hong, and R. Vahldieck, "Characterization of the propagation properties of the half-mode substrate integrated waveguide," *IEEE Trans. Microw. Theory Techn.*, vol. 57, no. 8, pp. 1996–2004, Aug. 2009.

[5] N. Grigoropoulos and P. R. Young, "Compact folded waveguides," in *Proc. 34th Eur. Microw. Conf.*, Amsterdam, The Netherlands, Oct. 2004, pp. 973–976.

[6] N. Grigoropoulos, B. Sanz-Izquierdo, and P. R. Young, "Substrate integrated folded waveguides (SIFW) and filters," *IEEE Microw. Wireless Compon. Lett.*, vol. 15, no. 12, pp. 829–831, Dec. 2005.

[7] W. Che, L. Geng, K. Deng, and Y. L. Chow, "Analysis and experiments of compact folded substrate-integrated waveguide," *IEEE Trans. Microw. Theory Techn.*, vol. 56, no. 1, pp. 88–93, Jan. 2008.

[8] M. Bozzi, S. A. Winkler, and K. Wu, "Broadband and compact ridge substrate-integrated waveguides," *IET Microw. Antennas Propag.*, vol. 4, no. 11, pp. 1965–1973, 2010.

[9] M. Coulombe, H. V. Nguyen, and C. Caloz, "Substrate integrated artificial dielectric (SIAD) structure for miniaturized microstrip circuits," *IEEE Antennas Wireless Propag. Lett.*, vol. 6, pp. 575–579, 2007.

[10] N. Yang, C. Caloz, and K. Wu, "Lowpass filter with slow-wave rail coplanar stripline (R-CPS)," *Electron. Lett.*, vol. 45, no. 17, pp. 895–897, 2009.
[11] A.-L. Franc, E. Pistono, D. Gloria, and P. Ferrari, "High-performance shielded coplanar waveguides for the design of CMOS 60-GHz bandpass filters," *IEEE Trans. Electron Devices*, vol. 59, no. 5, pp. 1219–1226, May 2012.
[12] A. Niembro-Martín *et al.*, "Slow-wave substrate integrated waveguide," *IEEE Trans. Microw. Theory Techn.*, vol. 62, no. 8, pp. 1625–1633, Aug. 2014.
[13] H. Jin, K. Wang, J. Guo, S. Ding, and K. Wu, "Slow-wave effect of substrate integrated waveguide patterned with microstrip polyline," *IEEE Trans. Microw. Theory Techn.*, vol. 64, no. 6, pp. 1717–1726, Jun. 2016.
[14] H. Jin, Y. Zhou, Y. M. Huang, S. Ding, and K. Wu, "Miniaturized broadband coupler made of slow-wave half-mode substrate integrated waveguide," *IEEE Microw. Wireless Compon. Lett.*, vol. 27, no. 2, pp. 132–134, Feb. 2017.
[15] J. Li, C. Ding, F. Wei, and X. W. Shi, "Compact UWB BPF with notch band based on SW-HMSIW," *Electron. Lett.*, vol. 51, no. 17, pp. 1338–1339, 2015.
[16] H. Raether, "Surface plasmons on gratings," in *Surface Plasmons on Smooth and Rough Surfaces and on Gratings* (Springer Tracts in Modern Physics), vol. 111. Berlin, Germany: Springer, 1988, pp. 91–116.
[17] J. B. Pendry, L. Martín-Moreno, and F. J. Garcia-Vidal, "Mimicking surface plasmons with structured surfaces," *Science*, vol. 305, pp. 847–848, Aug. 2004.
[18] N. Talebi and M. Shahabadi, "Spoof surface plasmons propagating along a periodically corrugated coaxial waveguide," *J. Phys. D, Appl. Phys.*, vol. 43, no. 13, p. 135302, 2010.
[19] W. Q. Zhu, A. Agrawal, A. Cui, G. Kumar, and A. Nahata, "Engineering the propagation properties of planar plasmonic terahertz waveguides," *IEEE J. Sel. Topics Quantum Electron.*, vol. 17, no. 1, pp. 146–153, Jan./Feb. 2011.
[20] J. J. Wu, D. J. Hou, T. J. Yang, I. J. Hsieh, Y. H. Kao, and H. E. Lin, "Bandpass filter based on low frequency spoof surface plasmon polaritons," *Electron. Lett.*, vol. 48, no. 5, pp. 269–270, 2012.
[21] X. Shen, T. J. Cui, D. F. Martin-Cano, and J. Garcia-Vidal, "Conformal surface plasmons propagating on ultrathin and flexible films," *Proc. Nat. Acad. Sci. USA*, vol. 110, no. 1, pp. 40–45, Jan. 2013.
[22] H. F. Ma, X. Shen, Q. Cheng, W. X. Jiang, and T. J. Cui, "Broadband and high?efficiency conversion from guided waves to spoof surface plasmon polaritons," *Laser Photon. Rev.*, vol. 8, no. 1, pp. 146–151, 2014.
[23] A. Kianinejad, Z. N. Chen, and C.-W. Qiu, "Low-loss spoof surface plasmon slow-wave transmission lines with compact transition and high isolation," *IEEE Trans. Microw. Theory Techn.*, vol. 64, no. 10, pp. 3078–3086, Oct. 2016.
[24] A. Kianinejad, Z. N. Chen, and C.-W. Qiu, "Design and modeling of spoof surface plasmon modes-based microwave slow-wave transmission line," *IEEE Trans. Microw. Theory Techn.*, vol. 63, no. 6, pp. 1817–1825, Jun. 2015.
[25] X. Gao, L. Zhou, Z. Liao, H. F. Ma, and T. J. Cui, "An ultra-wideband surface plasmonic filter in microwave frequency," *Appl. Phys. Lett.*, vol. 104, no. 19, p. 191603, 2014.
[26] J. Y. Yin, J. Ren, H. C. Zhang, B. C. Pan, and T. J. Cui, "Broadband frequency-selective spoof surface plasmon polaritons on ultrathin metallic structure," *Sci. Rep.*, vol. 5, Feb. 2015, Art. no. 8165.
[27] D.-F. Guan, P. You, Q. Zhang, Z.-H. Lu, S.-W. Yong, and K. Xiao, "A wide-angle and circularly polarized beam-scanning antenna based on microstrip spoof surface plasmon polariton transmission line," *IEEE Antennas Wireless Propag. Lett.*, vol. 16, pp. 2538–2541, 2017.
[28] A. Kianinejad, Z. N. Chen, and C.-W. Qiu, "A single-layered spoof-plasmon-mode leaky wave antenna with consistent gain," *IEEE Trans. Antennas Propag.*, vol. 65, no. 2, pp. 681–687, Feb. 2017.
[29] A. Kianinejad, Z. N. Chen, L. Zhang, W. Liu, and C.-W. Qiu, "Spoof plasmon-based slow-wave excitation of dielectric resonator antennas," *IEEE Trans. Antennas Propag.*, vol. 64, no. 6, pp. 2094–2099, Jun. 2016.
[30] D.-F. Guan, P. You, Q. Zhang, K. Xiao, and S.-W. Yong, "Hybrid spoof surface plasmon polariton and substrate integrated waveguide transmission line and its application in filter," *IEEE Trans. Microw. Theory Techn.*, vol. 65, no. 12, pp. 4925–4932, Dec. 2017.

Authors' photographs and biographies not available at the time of publication.